Direct methane-to-ethylene conversion in a nanosecond pulsed discharge

M. Scapinello[†], E. Delikonstantis[†] and G. D. Stefanidis[*]

Process Engineering for Sustainable Systems (ProcESS), Department of Chemical Engineering KU Leuven, Celestijnenlaan 200F, 3001 Leuven, Belgium

Abstract

We report that gas phase plasma-assisted non-oxidative methane coupling can lead to formation of ethylene as major product at ~20 % yield per pass. This is attained by using a nanosecond pulsed discharge (NPD) reactor, featuring rapid product quenching rates, (recyclable) hydrogen co-feeding (CH_4:H_2=1:1) and elevated pressures (5 bar) at which NPD is ignited.

1. Introduction

The societal and industrial importance of methane, as a source of energy and chemicals, in the coming decennia will be significant. The enormous reserves found (proven world natural gas reserves were $187x10^{12}$ m3 for the year 2016 [1] in addition to 10^{15} to 10^{18} m3 of methane stored in hydrates [2]), environmental sustainability and lower overall costs point to natural gas as the primary source for energy and chemicals in the near future. The great variety of methane sources, including existing gas networks, small natural gas fields, shale gas, coal beds, agricultural biogas and deep-sea methane hydrates creates

[*] Corresponding author. E-mail address: georgios.stefanidis@kuleuven.be
[†] The authors have equally contributed to this work

an urgent need to develop modular and flexible reactor systems able to valorize methane to chemicals or liquid fuels and to operate with changing methane feedstock in various environments.

Methane can be converted to methanol and synthetic fuels via syngas, or directly to olefins. These processes are not directly competitive; depending on the location, the available process and transportation infrastructure, the magnitude of available methane resources, the presence of other chemical feeds (e.g., CO_2) and current market value of relevant products, different valorization routes may be selected. Considering the products above, ethylene has the highest market value since it is the basic building block for a very broad range of chemicals ranging from plastics to solvents. Therefore, simple, scalable and efficient processes to convert methane to ethylene are highly desired. Direct methane transformation to ethylene may occur via oxidative or non-oxidative coupling. Oxidative coupling is exothermic and occurs at 1000-1200 K in presence of catalyst (metal oxides) and oxygen. However, the low single-pass C_2 yields of 18-26 % [3] (while commercial viability requires ethylene yields > 25 %), high purity O_2 demand and by-products formation (CO_2, CO, H_2 and H_2O), which necessitate intensive downstream processing, have limited the exploitation potential of the technology so far. Non-oxidative methane coupling results in light hydrocarbons (mainly C_2 species), hydrogen, carbon, benzene and other aromatics depending on the process conditions (mainly temperature and catalyst type). Carbon and hydrogen are thermodynamically the most stable products in the temperature range 1000-3300 K. In addition, benzene is formed in the temperature range 1100-1500 K while mainly acetylene is formed at higher temperatures [4]. Ethylene formation is maximized in the range 1300-1800 K [4]. Recently, Guo et al. synthesized an iron-based catalyst (Fe/SiO_2) that enables direct non-oxidative methane coupling at 1363 K and yield of 23.4 % [5].

Alternative technologies for methane processing at low temperatures have also been investigated aiming at improved energy efficiency, catalyst stability and process safety. Among them, non-thermal plasma can activate methane coupling and reforming reactions at lower temperatures, overcoming the thermal losses

in gas heating [6]. Concerning methane coupling, plasma is not very selective to ethylene. Ethane is mainly formed in dielectric barrier discharges (DBD) [7], or other low energy density discharges, while acetylene and carbon are the dominant products in high energy density discharges (MW [8], GA [9], spark [10] and corona [11]). Long chain hydrocarbons can also be formed under specific conditions (in batch DBD) [12]. Relatively high ethylene selectivity, comparable to that of acetylene and ethane, can only be obtained in glow discharges [13]. The reason of the different product distributions obtained from different types of plasma discharges is essentially the different plasma chemistries that are determined by the plasma characteristics. In DBD and low energy density discharges, electron impact reactions drive the reactivity, leading to CH_3 radical formation in the discharge [14] and consequently to ethane and propane after CH_3 radical recombination reactions at low temperatures [15]. By increasing the reduced electric field, the fragmentation pattern is shifted from CH_3 to CH_2, CH and C radicals [16]. Since the energetic thresholds of these electron impact reactions are comparable, no remarkable enrichment of CH_2 radicals (ethylene precursors) is attained and thus, ethylene formation is limited. In high energy density discharges or "warm" discharges, apart from the electron impact reactions, high temperatures (from hundreds to thousands of degrees Celsius) can further promote methane conversion and dehydrogenation reactions to acetylene and carbon [17]. It is possible to kinetically control carbon formation since methane coupling and dehydrogenation reactions proceed sequentially (methane → ethane → ethylene → acetylene → carbon). Ethylene formation requires 10^{-6}-10^{-5} s, while acetylene 10^{-5}-10^{-4} s [18]. Conventional quenching systems cannot achieve very fast quenching rates to suppress ethylene dehydrogenation to acetylene. A relatively new plasma technology in the field of chemical processing, the Nanosecond Pulsed Discharge (NPD) technology can achieve higher quenching rates; Lotfalipour et al. [19] has calculated the quenching rate to be ~20 K μs^{-1}, that is 20 times higher than in conventional systems (i.e. Hüels process). Martini and coworkers measured the quenching rate in CO_2 splitting (7.5 K μs^{-1}) using LIF spectroscopy [20].

NPD is generated using a nanosecond pulsed power supply unit, with voltage rise rate in the order of kV ns^{-1} or higher and pulse duration in the range of tens of ns [21]. At these conditions, arc is prevented and non-equilibrium plasma is sustained. In the case of methane coupling, the streamer-to-spark regime may be significant; the discharge includes a streamer that propagates between the electrodes followed by a spark in the active channel. The temperature of the active channel during the discharge rapidly increases and reaches thousands of degrees Kelvin in few tens of ns, activating also thermally driven reactions. This fast heating rate is not a requirement in methane coupling but the ability to reach high temperatures does affect the chemistry; methane can be dehydrogenated by H radicals at 1000 K and dehydrogenation of ethane to ethylene and ethylene to acetylene can be activated by H radicals at 1300 K [17]. Collectively, both methane conversion and unsaturated hydrocarbons selectivity increase. Higher temperatures are avoided as they lead to significant amounts of carbon.

In this work, we present the results of methane coupling using a nanosecond pulsed discharge in a coaxial reactor. We particularly investigate, for first time, the combined effect of the hydrogen content in the feed and the plasma reactor pressure and we show that proper selection of these parameter values in combination with the unique features of the NPD technology can lead to remarkable ethylene yields through single-step plasma processing, unlike previous important works in the field in which acetylene was the major product [19],[22]. Since the aim of the work is the production of ethylene as main product, we have focused on determination of the C_2 species, which represent the products of the main reactivity at the studied experimental conditions. The results of the current work are also compared to other pioneering works, in which ethylene was produced from methane and considerable yields were attained.

2. Materials and methods

A detailed schematic representation of the experimental setup used is presented in *Figure 1*. The plasma reactor is a coaxial shaped reactor that comprises an inner axial wire and an outer co-axial tube. The inner

axial wire constitutes the high voltage (HV) electrode of the reactor; it is made of copper with a diameter of 2.2 mm. The outer coaxial tube constitutes the ground electrode (GE) of the reactor; it is made of stainless steel with 7 mm ID, 10 mm OD and nominal gap (distance between the HV and the ground electrode) of 2.4 mm. The coaxial plasma reactor is 25 cm long.

The discharge is generated by a nanosecond pulsed power supply (n-PS) (NPG-24/2500, Megaimpulse Ltd.), and is triggered by a waveform generator (WFG) (33220A, Keysight Technology) at a frequency of 3000 Hz. The applied voltage and discharge current are measured by using a high-voltage probe (P6015A, Tektronix) and an I/V converter (CT-D-1.0, Magnelab) respectively. The voltage and current signals are continuously recorded with a frequency of 10 GS/s by a digital oscilloscope (Wavesurfer 10, Teledyne Lecroy). The energy input into the discharge is estimated as in previous work [23]. The time delay between the voltage (V) and current (I) signals is calculated by zeroing the time integral of V×I product, under no breakdown conditions (absence of discharge), achieved by filling the plasma reactor with SF_6 [24]. A typical signal time delay is 2.8 ± 0.2 ns. The integral of the instantaneous power (V×I) corrected by the delay over the time defines the pulse energy.

Two mass flow controllers (GF40 Series, Brooks Instrument) are employed to control the feed flowrate of the reactants (CH_4, Airliquide 99.995 % purity, and H_2, Airliquide 99.999 % purity). At the plasma reactor outlet flow, a filter (SS-4TF-7, Swagelok) with 7-micron pore size is placed to remove the formed carbonaceous powder. A differential pressure meter (Model 700.02, WIKA) monitors the increase in differential pressure (due to clogging of the filter) across the filter cloth. When the differential pressure exceeds a certain value, the outlet plasma reactor flow is driven through a second (clean) identical filter while the first one is cleaned. Working with clean filters is essential in order to keep the same operating pressure inside the plasma reactor. Clogged filters lead to pressure rise inside the plasma reactor chamber. A pressure flow controller (SLA5820, Brooks Instrument) is employed to precisely control the plasma reactor pressure when the effect of the operating pressure is investigated in the range 1-5 bar,

chosen for safety and plasma stability reasons. A third mass flow controller (GF40 Series, Brooks Instrument), which is operated as flowmeter, continuously records the volumetric flowrate of the plasma reactor outflow. The readout value depends on a gas factor, which varies with the gas composition. The gas composition is not constant over the course of the plasma reaction though. To accurately measure the value of the outflow, N_2 (Airliquide, 99.999 % purity) is fed into the plasma reactor outlet flow (not inside the plasma zone), right after the filter, acting as internal standard [25]. The outflow rate is obtained by multiplying the initial total flowrate (CH_4 + H_2 + N_2) by the ratio of the chromatographic area of N_2 before and during the discharge. A fourth mass flow controller (4800 series, Brooks Instrument) is used to control the flow of N_2, which is used as internal standard. Pressure probes (P1600 and P1650, Pace Scientific) and thermocouples (PT 900 Pace scientific) monitor the pressure and temperature values prior to the reactor and the gas chromatography equipment (GC).

The plasma reactor outflow is analyzed using an on-line GC (3000 MicroGC, Inficon). A Molesieve column (10 m) with backflush (3 m, Plot U) is employed to detect H_2, N_2, CH_4; a Plot U column (10 m) with backflush (1 m, Plot Q) is used to detect C_2H_4, C_2H_6, C_2H_2, C_3H_8, C_3H_6 and C_3H_4 and an Alumina column (10 m, 0.32 mm) with backflush (1 m, 0.32 mm, Alumina) is used to detect C_4-C_6 products.

Prior to the discharge initiation, the plasma reactor chamber is flushed with the reactants for about 30 min to remove the trapped air and stabilize and measure the initial composition of the feed. Immediately after plasma ignition, instability in plasma performance is observed for the first five minutes. Afterwards, steady-state conditions are reached and the discharge is sustained for 30 minutes. The reported results include only data obtained during the steady-state period. Longer runs (up to 2 hours) revealed a slight decrease in the plasma reactor performance, apparently due to carbon accumulation on the electrodes.

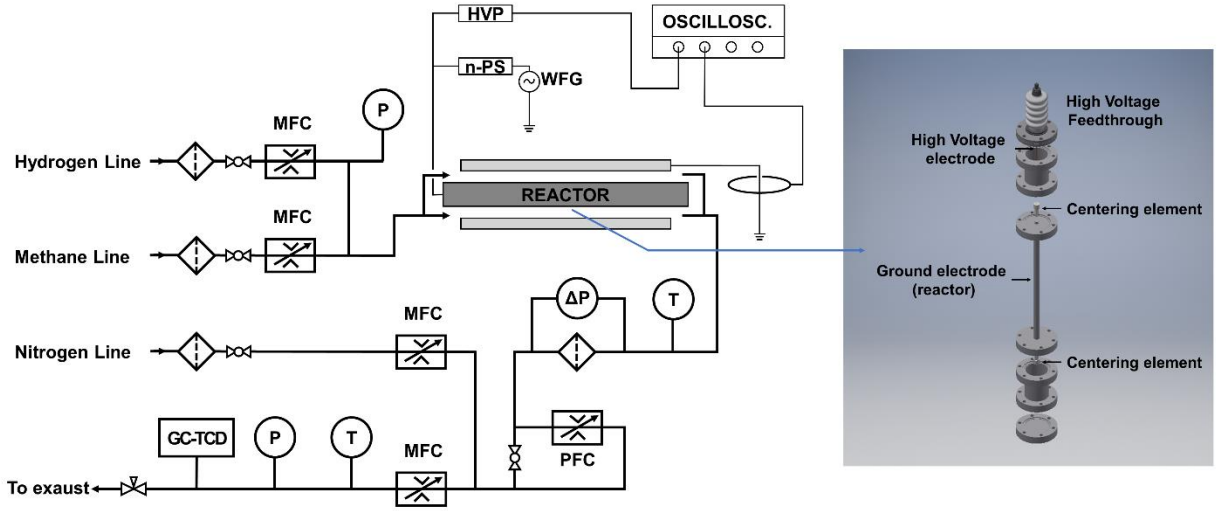

Figure 1 Representative drawing of the experimental setup: MFC, mass flow controllers; PFC, pressure flow controller; WFG, waveform generator; n-PS, nanosecond pulsed generator; HVP, high voltage probe; OSCILLOSC, oscilloscope; GC-TCD, gas chromatography with thermal conductivity detector; P, pressure probes; ΔP, differential pressure meter; T, thermocouples.

For the evaluation of the process performance, we calculate the conversion (Eq. 1) and the selectivity (Eq. 2), as following:

$$CH_4 \text{ conversion } [\%] = \left(1 - \frac{[CH_4]' \times V'}{[CH_4]^0 \times V^0}\right) \times 100 \qquad \text{(Eq. 1)}$$

$$C_2H_x \text{ selectivity } [\%] = \left(\frac{2 \times [C_2H_x]' \times V'}{[CH_4]^0 \times V^0 - [CH_4]' \times V'}\right) \times 100 \qquad \text{(Eq. 2)}$$

where $[\ldots]^0$ and $[\ldots]'$ are the concentrations of CH_4 at the plasma reactor inflow and outflow obtained by the on-line GC analysis, while V^0 and V' are the respective volumetric flowrates. The yield of C_2 compounds (Eq. 3) is defined as the product of methane conversion and the selectivity to the respective compound:

$$C_2H_x \text{ yield } [\%] = \frac{CH_4 \text{ conversion} \times C_2H_x \text{ selectivity}}{100} \qquad \text{(Eq. 3)}$$

The carbon balance is expressed as carbon lack, and described by Eq. 4:

$$C \text{ lack } [\%] = \left(1 - \frac{V' \times \left([CH_4]' + 2 \times \left([C_2H_2]' + [C_2H_4]' + [C_2H_6]'\right)\right)}{V^0 \times [CH_4]^0}\right) \times 100 \quad \text{(Eq. 4)}$$

This parameter includes the contributions of the carbon powder deposited on the walls of the reactor and the heavier species (C_3-C_6), which are detected by the GC, but not quantified.

To evaluate the energy performance of the plasma reactor, the specific energy input (SEI), the specific energy requirement (SER) and the energy cost for ethylene formation (EC) are calculated. SEI defines the channeled energy per mole of methane contained in the feed. The mathematical expression of SEI is described by Eq. 5:

$$\mathrm{SEI}\left[\mathrm{kJ\ mol_{CH_4}^{-1}}\right] = \left(\frac{1344.84\ [\mathrm{s \times sccm \times mol^{-1}}] \times E_{pulse}\ [\mathrm{J}] \times f\ [\mathrm{Hz}]}{V^{0}_{CH_4}\ [\mathrm{sccm}]}\right) \quad \text{(Eq. 5)}$$

SER defines the energy required for the conversion of 1 mole of methane. The mathematical expression of SEI is described by Eq. 6:

$$\mathrm{SER}\left[\mathrm{kJ\ mol_{CH_4}^{-1}}\right] = \frac{\mathrm{SEI} \times 100}{\mathrm{CH_4\ conversion\ [\%]}} \quad \text{(Eq. 6)}$$

EC defines the amount of energy required for the production of 1 mole of ethylene through plasma-assisted methane coupling. The mathematical expression of SEI is described by Eq. 7:

$$\mathrm{EC}\left[\mathrm{kJ\ mol_{C_2H_4}^{-1}}\right] = \frac{2 \times \mathrm{SER} \times 100}{\mathrm{C_2H_4\ selectivity\ [\%]}} \quad \text{(Eq. 7)}$$

3. Results and discussion

In this work, the impact of the aforementioned advantages of NPD on methane coupling is investigated. A streamer-to-spark discharge is generated by a nanosecond pulsed power supply in the reactor and covers only ~3% of the hollow-cylindrical shaped volume around the discharge, defined by the streamer diameter and the plasma reactor cross-section area [19]. This concept of limited chemically active area compared to the reactor cross section area is what enables rapid product quenching and can tune product selectivity. The concept was effectively used in the prominent example of the short contact time catalytically coated gauge reactor that was used for direct partial oxidation of lower alkanes to olefins and other thermally labile oxygenate compounds [26]. In that work, rapid quenching of the hot intermediate products desorbed off the catalytically coated wires of the gauge reactor were rapidly quenched from 800°C to 400°C, at a rate of 2 K μs^{-1}, by mixing with the low temperature feed that passed unconverted

between the catalytically coated wires. In the current work, even higher quenching rates can be achieved combining the limited chemical active area with the repetitive ignition of a single nanosecond spark. Reactions may also occur around the plasma zone, at a distance longer than the discharge diameter, due to relatively high gas temperature [27].

Hydrogen addition to the feed generally suppresses carbon and benzene formation and increases acetylene selectivity at the expense of methane conversion in pyrolysis [28]; regarding ethylene production, no relevant information has been reported in [28] since the studied experimental conditions (residence time and temperature) promoted acetylene formation. The effect of hydrogen content in the feed on methane conversion and product distribution is presented in *Figure 2*. All experiments were run at a total feed rate of 200 sccm, frequency of 3 kHz, discharge gap of 2.4 mm and atmospheric pressure. The energy input was calculated at 5.7 ± 0.2 mJ/pulse for all CH_4:H_2 compositions and at 5.2 mJ/pulse for pure methane (due to higher breakdown voltage). The CH_4:H_2 composition varied between 1:0 to 1:3 molar ratio. Methane conversion decreases with increasing H_2 content (from 1:1 to 1:3) while acetylene (dominant product) selectivity increases, confirming the behavior observed in thermal pyrolysis [23]. The initial increment of conversion observed from 1:0 to 1:1 CH_4:H_2 ratio can be ascribed to the higher amount of energy channeled into the plasma in the case of equimolar methane/hydrogen feed (15.6 mJ/pulse; CH_4:H_2 = 1:0 versus 17.0 mJ/pulse; CH_4:H_2 =1:1). Ethylene and ethane selectivity remain almost constant.

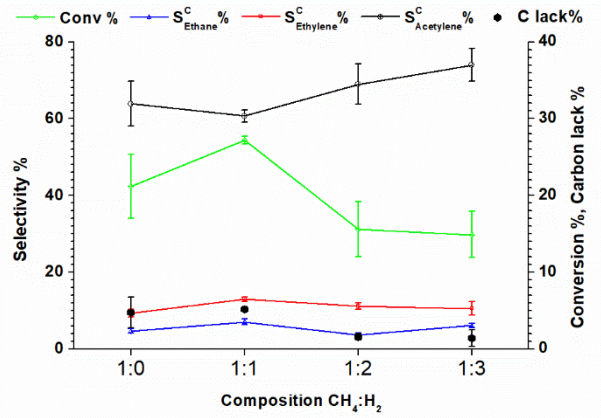

Figure 2. The effect of hydrogen content on methane conversion and product distribution in the plasma-assisted methane coupling process at atmospheric pressure. Total feed rate: 200 sccm, frequency: 3 kHz, discharge gap: 2.4 mm.

As reported in Table 1, at atmospheric pressure, the addition of hydrogen decreases the carbon lack, indicating that a lower amount of carbon and heavier species are produced compared to the case of pure methane. These results are aligned with the mechanism proposed by Kado et al. [24], who tried to explain the acetylene formation mechanism in spark discharges. They claimed that acetylene is produced through hydrogenation of atomic carbon and C_2 that are formed in high concentrations in spark discharges, rather than through methane coupling and sequential dehydrogenation (methane → ethane → ethylene → acetylene → carbon) as in warm discharges, where aside from electron impact reactions, the thermal effect can significantly affect the methane coupling reactions.

Table 1 Experimental data describing the plasma reactor performance; the errors represent the semi dispersion of the experimental values

Feed [sccm]		Pressure	Conversion	Selectivity %			Yield %			Carbon
H_2	CH_4	[bar_a]	%	C_2H_6	C_2H_4	C_2H_2	C_2H_6	C_2H_4	C_2H_2	Lack %
0	200	1.0	21±4	4.7±0.6	9.3±1.0	64±6	1.0±0.2	2.0±0.5	13.4±1.4	4.8±2.0
0	200	2.0	28.0±1.6	3.0±0.4	8.4±0.5	61.1±2.4	0.8±0.1	2.4±0.1	17.1±1.0	7.5±1.2
0	200	3.3	32.7±2.7	2.1±0.5	10.0±1.7	53±7	0.7±0.1	3.2±0.4	17±3.0	11.5±1.9
0	200	5.0	32.4±1.0	1.9±0.2	10.3±0.7	54±5	0.6±0.1	3.3±0.3	17.3±1.3	11.1±1.7
100	100	1.0	27.2±0.5	7.1±0.7	13.0±0.6	60.7±1.6	1.9±0.1	3.5±0.2	16.5±0.6	5.2±0.3
100	100	2.0	36±5	3.7±1.0	21±6	35±10	1.3±0.2	7.4±1.5	12±4	15±5
100	100	3.3	31.8±1.0	4.6±0.6	50±7	6.4±2.6	1.5±0.1	15.9±2.1	2.0±0.8	12.4±2.8
100	100	5.0	36.7±0.5	3.3±0.1	53±4	1.9±1.0	1.2±0.1	19.5±1.1	0.7±0.4	15.5±1.4
133	67	1.0	16±4	3.7±0.4	11.2±0.8	69±5	0.5±0.2	1.8±0.5	10.6±1.8	1.6±0.4
150	50	1.0	15±3	6.1±0.6	10.6±1.8	74±4	0.6±0.1	1.6±0.2	10.9±1.8	1.4±1.1
150	50	2.0	34.6±1.1	6.2±0.5	33.1±0.9	17.7±1.2	2.2±0.1	11.5±0.3	6.1±0.6	14.7±0.6
150	50	3.3	31.7±0.1	9.1±0.2	53.3±0.4	9.1±0.1	2.9±0.1	16.9±0.2	2.9±0.1	8.6±0.1
150	50	5.0	36.8±1.6	6.1±0.5	43.6±2.8	6±3	2.3±0.2	16.5±0.7	2.2±1.1	16.9±2.5

Pressure increase results in breakdown voltage increase since the electron mean free path is decreased due to higher molecule density. Thus, a stronger electric field is required to initiate and sustain the discharge [30]. The plasma active area is also reduced with pressure increase leading to lower current values (Table 2). Concurrently, pressure determines the electron-molecule collision frequency and the electron mean energy. Specifically, pressure increase results in a) more frequent collisions at higher

pressures, driving the system towards thermal equilibrium and b) lower electron mean energy, and thus less energetic collisions, as revealed by the decreasing reduced electric field (E/n max) at increasing pressure reported in Table 2. The effect of plasma reactor pressure on the methane coupling process is presented in *Figure 3*. Methane conversion initially increases from 21% to 32% as pressure increases from 1 to 3.3 bar due to the higher frequency of electron-molecule collisions. At 5 bar, methane conversion is similar to the one at 3.3 bar, due to the slightly lower discharge energy. Regarding product distribution, acetylene decreases while ethane and ethylene remain practically constant with pressure increase. In addition, the carbon lack increase with pressure increase, shown in Table 1, indicates promotion of polymerization and carbon production.

It is concluded that pressure increase alone does not promote ethylene formation, as expected by the lower energetic electron-molecule collisions.

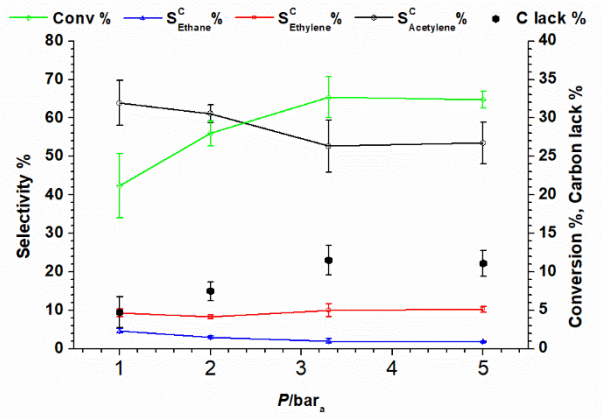

Figure 3. The effect of plasma reactor pressure on methane conversion and product distribution in the plasma-assisted methane coupling. Total feed rate: 200 sccm, frequency: 3 kHz, discharge gap: 2.4 mm. The CH_4:H_2 ratio is equal to 1:0.

Table 2 **.** Energy analysis of the plasma reactor; the required data were obtained from the electrical characterization of the discharge.

Feed [sccm]		Pressure	V_{max}[a]	I_{max}[a]	E pulse	Power	E/n max	SEI	SER	EC
H_2	CH_4	[bar_a]	[kV]	[A]	[mJ]	[W]	[Td]	[kJ/mol_{CH4}]	[kJ/mol_{CH4}]	[kJ/mol_{C2H4}]
0	200	1.0	14.3[b]	71.2[b]	15.6	5.2	244[b]	105	497	10800
0	200	2.0	19.1	75.7	18.2	6.1	163	122	437	10400
0	200	3.3	19.7	65.1	14.4	4.8	102	97	296	5910
0	200	5.0	20.6	69.1	14.5	4.8	70	98	302	5840
100	100	1.0	17.2	77.0	17.0	5.7	294	238	876	6740
100	100	2.0	17.9	74.4	15.5	5.2	153	210	586	5580
100	100	3.3	19.2	74.4	15.0	5.0	99	203	638	2550
100	100	5.0	19.6	66.4	13.9	4.6	67	196	532	2020
133	67	1.0	17.8	78.4	17.5	5.8	304	365	2350	42000
150	50	1.0	14.6	78.3	16.5	5.5	249	458	3080	58400
150	50	2.0	18.3	74.4	16.8	5.6	156	464	1340	8080
150	50	3.3	18.6	70.4	15.6	5.2	96	432	1350	5030
150	50	5.0	18.3	66.4	14.3	4.8	63	397	1080	4960

The combined effect of hydrogen content in the feed and plasma reactor pressure increase on the product distribution is presented in *Figure 4*. By increasing the amount of hydrogen up to 1:3 CH_4:H_2 and concurrently applying higher pressure than the atmospheric in the plasma reactor, product selectivity is shifted from acetylene to ethylene. At pressures > 3.3 bar, ethylene becomes the dominant product, while acetylene production is minimized (<3% yield). The highest ethylene yield (19.5%) is achieved at CH_4:H_2=1:1 and pressure 5 bar. At these conditions, acetylene yield is less than 1%, but the carbon lack gets a maximum value of ~17%, indicating that a higher amount of carbon and heavier species are produced. It is worth mentioning that no additional hydrogen source is required when the system is operated at steady state under the above mentioned conditions, since hydrogen is produced by methane cracking in the plasma zone. The amount of produced hydrogen exceeds the amount that need to be co-fed with methane into the plasma reactor to meet the targeted CH_4:H_2=1:1, but not ratios CH_4:H_2>1:1; in the latter case, additional hydrogen is required increasing the production cost. In the former case, the produced hydrogen can be separated from C_2 and other possible heavier species in a demethanizer,

[a] The reported voltage and current values correspond to the values measured immediately after the discharge ignition. These values are slightly higher than the values measured over the course of the discharge; therefore, they are called Vmax and Imax respectively. Carbon deposition on the electrodes during the plasma-assisted reaction affects the electrodes condition and results in lower applied voltages and lower currents

[b] Those values were measured at the end of the ran when carbon had already been deposited on the electrodes; therefore, those values are expected to be slightly higher

followed by a purification unit (pressure swing adsorption or membrane) to adjust the composition of CH_4:H_2 prior to recycling, while a pure hydrogen stream remains available to be utilized in other (integrated) processes or for energy production. Eventually, recycling part of the produced hydrogen back to the plasma reactor inlet can lead to a self-sustained system as regards hydrogen production and consumption.

Considering the current results from an industrial perspective, we remark that absence of catalyst results in mitigation of ethylene production cost and process complexity, while stable operation of the plasma reactor at elevated pressures facilitates easier process integration with gas storage, transportation infrastructure and ethylene purification units. Nevertheless, the current technology faces two main challenges namely, 1) formation of carbonaceous powder leading to reactor performance decrease and eventually to discharge suppression and 2) up-scaling issues associated with the nanosecond pulsed discharge itself. Carbonaceous powder is mitigated by hydrogen co-feed but not completely eliminated. Albeit cyclones implementation in the post plasma zone can enable carbonaceous powder removal, clogging issues and short-circuits in the plasma zone itself cannot be completely overcome. A smart reactor design may substantially tackle short-circuits initiation via a fast periodic cleaning operation. Up-scaling of the nanosecond pulsed discharge via replication of the operating module may be possible. In addition, recent developments in solid state switches may support the concurrent initiation of multiple plasma streamers powered by the same nanosecond power supply inside a single reactor volume. Then, parallel installation of such units can meet the industrially demanded throughputs.

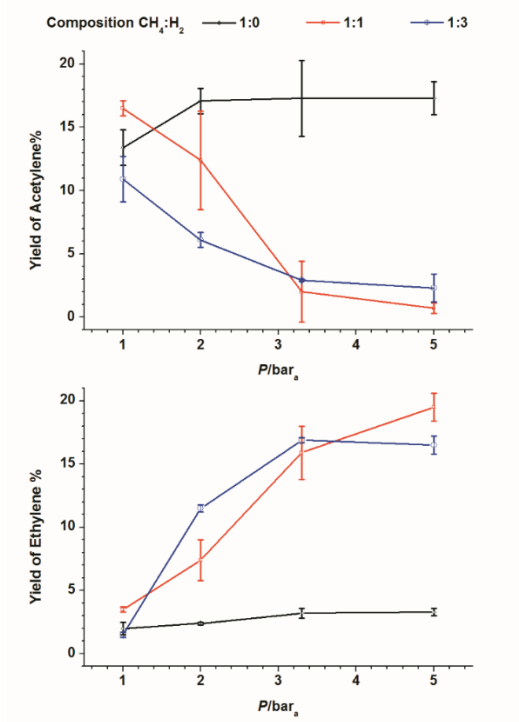

Figure 4. The combined effect of hydrogen content and plasma reactor pressure on methane conversion and product distribution in the plasma-assisted methane coupling process. Total feed rate: 200 sccm, frequency: 3 kHz, discharge gap: 2.4 mm.

The results herein differ substantially from those of thermal pyrolysis, where acetylene is the dominant product. The reason can be attributed to the high quenching rate in NPD between two consecutive voltage pulses, the increase in H radical concentration due to co-feeding of hydrogen in the discharge and the elevated pressure. H radicals can initiate the dehydrogenation reaction of methane at temperatures > 1000 K, enhancing methane conversion [17]. Pressure increase drives the system towards thermal equilibrium; therefore, the neutral species reach higher temperatures [30]. At temperatures higher than 1350 K, H radicals promote ethane-to-ethylene and ethylene-to-acetylene dehydrogenation reactions [17]. Fast quenching between the two abovementioned consecutive dehydrogenation reactions can suppress the second dehydrogenation reaction enhancing the ethylene selectivity [18].

For the pressure range studied herein (1-5 bar), it can be concluded that EC decreases monotonically with increasing pressure and thereby increasing ethylene yield. As regards the effect of H_2 in the feed, however, the minimum EC is obtained at the intermediate concentration ratio CH_4:H_2=1:1; high dilution of methane

in hydrogen (CH_4:H_2=1:3) has a negative effect on EC. Further improvement can possibly be expected at pressures higher than 5 bar, provided sufficient power input to ignite the discharge, and at more extended discharge cross section areas. Finally, comparison with other plasma processes is not simple as ethylene has always been produced as by-product at low concentrations. Nonetheless, in Table 3, we quote the articles with the highest reported ethylene yields up to now.

Table 3. Comparison of the highest reported ethylene yields produced directly from methane, without use of catalyst, with the current work.

Plasma Technology	Pressure [bar_a]	SEI [kJ/mol]	Conversion %	Selectivity C_2H_4 %	Yield C_2H_4 %	EC [kJ/mol C_2H_4]	Ref.
Microwave	1.5	1613	52.5	28.1	14.8	21980	[31]
Microwave	0.1	1075	92	9	8.3	25900	[32]
Current	5.0	196	36.7	52.8	19.5	2020	

4. Conclusions

Nanosecond pulsed discharge (NPD) is an efficient technology for direct methane coupling to ethylene. Nearly 20% ethylene yield is attained when application of NPD is combined with elevated pressures (5 bar) and hydrogen in the feed (CH_4:H_2=1:1). This yield is the highest that has been achieved with plasma technology and close to the recently published state-of-the-art in the field using conventional thermal catalysis (23.4% ethylene yield at 1363 K)[5]. Compared to the latter work though, the advantages of the plasma process reported herein are that no catalyst is necessary, the exit bulk gas temperature is relatively low (650-750 K) and the technology is directly compatible with the emerging concept of powering chemical reactors using renewable electricity.

5. Acknowledgements

This work has received funding from the European Union's Horizon 2020 Research and Innovation Programme through project "Adaptable Reactors for Resource and Energy Efficient Methane Valorization" (ADREM), No. 680777.

6. References

[1] BP Statistical Review of World Energy June 2017, British Petroleum p.l.c. Available online: bp.com/statisticalreview (accessed on 22 november 2017).

[2] T. S. Collett, A. H. Johnson, C. C. Knapp and R. Boswell, in Natural Gas Hydrates - Energy Resources Potential and Associated Geologic Hazards. AAPG Memoir 89., eds. T. S. Collett, A. H. Johnson, C. C. Knapp and R. Boswell, AAPG, 2009, 146–219.

[3] Karakaya C, Kee RJ. Progress in the direct catalytic conversion of methane to fuels and chemicals. Prog Energy Combust Sci 2016;55:60–97.

[4] Fincke JR, Anderson RP, Hyde TA, Detering BA. Plasma Pyrolysis of Methane to Hydrogen and Carbon Black. Ind Eng Chem Res 2002;41:1425–35.

[5] Guo X, Fang G, Li G, Ma H, Fan H, Yu L, et al. Direct, Nonoxidative Conversion of Methane to Ethylene, Aromatics, and Hydrogen. Science 2014;344:616–9.

[6] Scapinello M, Delikonstantis E, Stefanidis GD. The panorama of plasma-assisted non-oxidative methane reforming. Chem Eng Process Process Intensif 2017;117:120–40.

[7] Liu SY, Mei DH, Shen Z, Tu X. Nonoxidative conversion of methane in a dielectric barrier discharge reactor: Prediction of reaction performance based on neural network model. J Phys Chem C 2014;118:10686–93.

[8] Heintze M, Magureanu M, Kettlitz M. Mechanism of C2 hydrocarbon formation from methane in a pulsed microwave plasma. J Appl Phys 2002;92:7022–31.

[9] Zhang H, Du C, Wu A, Bo Z, Yan J, Li X. Rotating gliding arc assisted methane decomposition in nitrogen for hydrogen production. Int J Hydrogen Energy 2014;39:12620–35.

[10] Shapoval V, Marotta E. Investigation on plasma-driven methane dry reforming in a self-triggered spark reactor. Plasma Process Polym 2015;12:808–16.

[11] Beloqui Redondo A, Troussard E, Van Bokhoven JA. Non-oxidative methane conversion assisted by

corona discharge. Fuel Process Technol 2012;104:265–70.

[12] Scarduelli G, Guella G, Mancini I, Dilecce G, De Benedictis S, Tosi P. Methane oligomerization in a dielectric barrier discharge at atmospheric pressure. Plasma Process Polym 2009;6:27–33.

[13] Yang Y. Methane Conversion and Reforming by Nonthermal Plasma on Pins. Ind Eng Chem Res 2002;41:5918–26.

[14] Nozaki T, Okazaki K. Non-thermal plasma catalysis of methane: Principles, energy efficiency, and applications. Catal Today 2013;211:29–38.

[15] De Bie C, Verheyde B, Martens T, Van Dijk J, Paulussen S, Bogaerts A. Fluid modeling of the conversion of methane into higher hydrocarbons in an atmospheric pressure dielectric barrier discharge. Plasma Process Polym 2011;8:1033–58.

[16] Nozaki T, Hattori A, Okazaki K. Partial oxidation of methane using a microscale non-equilibrium plasma reactor. Catal. Today 2004;98:607–16.

[17] Ravasio S, Cavallotti C. Analysis of reactivity and energy efficiency of methane conversion through non thermal plasmas. Chem Eng Sci 2012;84:580–90.

[18] Fincke JR, Anderson RP, Hyde T, Detering BA, Wright R, Bewley RL, et al. Plasma Thermal Conversion of Methane to Acetylene. Plasma Chem Plasma Process 2002;22:105–36.

[19] Lotfalipour R, Ghorbanzadeh AM, Mahdian A. Methane conversion by repetitive nanosecond pulsed plasma. J Phys D Appl Phys 2014;47.

[20] Martini LM, Gatti N, Dilecce G, Scotoni M. Laser induced fluorescence in nanosecond repetitively pulsed discharges for CO2 conversion. Plasma Phys Control Fusion 2018;60:14016.

[21] Starikovskaia SM. Plasma assisted ignition and combustion. J Phys D Appl Phys 2006;39.

[22] Yao SL, Suzuki E, Meng N, Nakayama A. Influence of rise time of pulse voltage on the pulsed plasma conversion of methane. Energy Fuels 2001;15:1300–3.

[23] Scapinello M, Martini LM, Dilecce G, Tosi P. Conversion of CH4 /CO2 by a nanosecond repetitively

pulsed discharge. J Phys D Appl Phys 2016;49.

[24] Takashima (Udagawa) K, Zuzeek Y, Lempert WR, Adamovich I V. Characterization of a surface dielectric barrier discharge plasma sustained by repetitive nanosecond pulses. Plasma Sources Sci Technol 2011;20:55009.

[25] Lee R, Labrecque R, Lavoie J-M. Inline Analysis of the Dry Reforming Process through Fourier Transform Infrared Spectroscopy and Use of Nitrogen as an Internal Standard for Online Gas Chromatography Analysis. Energy Fuels 2014;28:7398–402.

[26] Goetsch D a., Schmidt LD. Microsecond Catalytic Partial Oxidation of Alkanes. Science 1996;271:1560–2.

[27] Lo A, Cessou A, Lacour C, Lecordier B, Boubert P, Xu DA, et al. Streamer-to-spark transition initiated by a nanosecond overvoltage pulsed discharge in air. Plasma Sources Sci Technol 2017;26.

[28] Holmen A, Olsvik O, Rokstad OA. Pyrolysis of natural gas: chemistry and process concepts. Fuel Process Technol 1995;42:249–67.

[29] Kado S, Urasaki K, Sekine Y, Fujimoto K, Nozaki T, Okazaki K. Reaction mechanism of methane activation using non-equilibrium pulsed discharge at room temperature. Fuel 2003;82:2291–7.

[30] A. A. Fridman, Plasma Chemistry, 2008, 598- 603, 157-159, 192.

[31] Zhang J-Q, Yang Y-J, Zhang J-S, Liu Q, Tan K-R. Non-oxidative Coupling of Methane to C2 Hydrocarbons under Above-atmospheric Pressure Using Pulsed Microwave Plasma. Energy Fuels 2002;16:687–93.

[32] Shen C, Sun Y, Sun D, Yang H. A study on methane coupling to acetylene under the microwave plasma. Sci China Chem 2010;53:231–7.